The Astronomical Journal, 131:889–894, 2006 February

A RADIO AND X-RAY STUDY OF HISTORICAL SUPERNOVAE IN M83

Christopher J. Stockdale,[1] Larry A. Maddox,[2] John J. Cowan,[2] Andrea Prestwich,[3]
Roy Kilgard,[3] and Stefan Immler[4]

Received 2004 December 27; accepted 2005 October 25

ABSTRACT

We report the results of 15 years of radio observations of the six historical supernovae (SNe) in M83 using the Very Large Array. We note the near-linear decline in radio emission from SN 1957D, a Type II SN, which remains a nonthermal radio emitter. The measured flux densities from SNe 1923A and 1950B have flattened as they begin to fade below detectable limits; they are also Type II SNe. The luminosities for these three SNe are comparable with the radio luminosities of other decades-old SNe at similar epochs. SNe 1945B, 1968L, and 1983N were not detected in the most recent observations, and these nondetections are consistent with previous studies. We report the X-ray nondetections of all six historical SNe using the *Chandra X-Ray Observatory*, consistent with previous X-ray searches of other decades-old SNe and low inferred mass-loss rates of the progenitors [$\dot{M} \approx (10^{-8}\ M_{\odot}\ \mathrm{yr}^{-1})(v_w/10\ \mathrm{km\ s}^{-1})$].

Key words: galaxies: individual (M83) — radio continuum: galaxies — supernovae: general — supernovae: individual (SN 1923A, SN 1945B, SN 1950B, SN 1957D, SN 1968L, SN 1983N)

1. INTRODUCTION

M83, an SABc galaxy, is a typical grand design, face-on spiral galaxy with an inclination of 24° (Talbot et al. 1979). It is relatively nearby, with distance estimates ranging from 3.75 Mpc (de Vaucouleurs 1979) to 8.9 Mpc (Sandage & Tammann 1987). We have opted to use the Cepheid-established distance of 4.5 Mpc (Thim et al. 2003). The close proximity and low inclination of M83, along with six optically discovered supernovae (SNe), make it an ideal system for studying extragalactic SNe at all wavelengths. Here we report on a radio and X-ray study of six historical SNe.

Using the Very Large Array (VLA),[5] radio observations have detected emission from four historical SNe, SNe 1923A, 1950B, 1957D, and 1983N (Cowan & Branch 1982, 1985; Cowan et al. 1994; Sramek et al. 1984), while two others, SNe 1945B and 1968L, have not been detected in the radio. SN 1968L lies within the bright, diffuse, radio nuclear emission and would not have been detectable unless it was extremely radio bright. This 20 year study of M83 by Cowan and collaborators has yielded an insight into the evolution of the long-term transient sources in M83, primarily SNe, supernova remnants (SNRs), and its nucleus. Chevalier (1984) proposes that synchrotron radiation is produced in the region of interaction between the SN blast wave and the circumstellar shell that originated from the prior mass loss of the progenitor star. In such models, the emission fades as the density of the circumstellar material (CSM) decreases. Cowsik & Sarkar (1984) suggest a minimum of 100 yr before the radio emission rebrightens when the blast wave begins to encounter the interstellar medium, as the source evolves into a SNR. Cowan et al. (1994) charted the evolution of 14 of the brightest radio sources over the course of 10 years at 6 and 20 cm. We have reanalyzed the Cowan et al. (1994) results and discovered at least 5 times the number of discrete radio sources in M83; the complete discussion will be presented in L. A. Maddox et al. (2006, in preparation). Immler et al. (1999) detected 37 discrete X-ray sources in M83 with *ROSAT* observations, but no radio emission was detected from the historical SNe.

In this paper we report new radio observations of the historical SNe of M83, including their current flux densities, spectral indices, and decay indices, examining how their radio emission has varied during the time that they have been monitored. We also give upper limits to the X-ray flux for the historical SNe.

2. OBSERVATIONS

2.1. *Radio*

The new VLA observations of M83 were made with four observing runs. In the first two, M83 was observed for 8.7 total hr on 1998 June 13 and 15, at 20 cm (1.450 GHz) using the VLA in its BnA configuration (the southern arms in the B configuration and the northern arm in the A configuration), with a maximum baseline of 24 km. During the second group of observing runs, M83 was observed on 1998 October 31 and November 1 with the VLA in its CnB configuration (maximum baseline of ∼11 km) at 6 cm (4.860 GHz) for a total of 8.9 hr. These were done using two 25 MHz bands in dual polarization, split into eight spectral channels each. For the purposes of this study, we are only interested in the continuum observations of the SNe and have only analyzed the channel 0, "pseudocontinuum" data that utilize 75% of the 50 MHz bandwidth in each of the two orthogonal circular polarizations. The phase calibrator was J1316−336, with 3C 286 used to set the flux density scale. In each observation, the pointing center was $13^{\mathrm{h}}37^{\mathrm{m}}00^{\mathrm{s}}.22$, $-29^{\circ}52'04''.5$ (J2000.0).

Data were Fourier transformed and deconvolved using the CLEAN algorithm as implemented in the Astronomical Image Processing System (AIPS) routine SCIMG. The data were weighted using Brigg's robustness parameter of 0, which minimizes the point-spread function while maximizing sensitivity. In addition, SCIMG implements a self-calibration algorithm to reduce the

[1] Department of Physics, Marquette University, P.O. Box 1881, Milwaukee, WI 53201-1881; christopher.stockdale@marquette.edu.
[2] Homer L. Dodge Department of Physics and Astronomy, University of Oklahoma, 440 West Brooks, Room 131, Norman, OK 73019; maddox@nhn.ou.edu, cowan@nhn.ou.edu.
[3] Harvard-Smithsonian Center for Astrophysics, 60 Garden Street, Cambridge, MA 02138; aprestwich@cfa.harvard.edu, rkilgard@cfa.harvard.edu.
[4] Exploration of the Universe Division, X-Ray Astrophysics Laboratory, Code 662, NASA Goddard Space Flight Center, Greenbelt, MD 20771; immler@milkyway.gsfc.nasa.gov.
[5] The VLA telescope of the National Radio Astronomy Observatory is operated by Associated Universities, Inc., under a cooperative agreement with the National Science Foundation.

TABLE 1

RADIO FLUX DENSITIES AND UPPER LIMITS TO THE X-RAY LUMINOSITY FOR HISTORICAL SNe IN M83

	Position		1998 Flux Densities			1990–1992 Flux Densities			
Source SN	R.A. (J2000.0)	Decl. (J2000.0)	20 cm (mJy)	6 cm (mJy)	Spectral Index	20 cm (mJy)	6 cm (mJy)	Spectral Index	L_X[a] (ergs s^{-1})
1957D.....	13 37 03.57	−29 49 40.6	0.73 ± 0.09	0.64 ± 0.05	-0.11 ± 0.15	1.75 ± 0.07	1.50 ± 0.04	-0.13 ± 0.06	2.2×10^{36}
1950B.....	13 36 52.08	−29 51 55.7	0.50 ± 0.05	0.47 ± 0.04	-0.05 ± 0.13	0.52 ± 0.05	0.49 ± 0.04	-0.05 ± 0.13	1.4×10^{36}
1923A.....	13 37 09.31	−29 51 00.7	≤ 0.15	0.21 ± 0.04	≥ 0.28	0.17 ± 0.05	0.21 ± 0.03	$+0.18 \pm 0.33$	2.2×10^{36}
1983N.....	13 36 50.31	−29 54 02.3	≤ 0.15	≤ 0.12	...	...	...	...	1.7×10^{36}
1945B.....	13 36 51	−30 10 17	≤ 0.15	≤ 0.12	...	...	...	...	3.6×10^{36}

NOTES.—Units of right ascension are hours, minutes, and seconds, and units of declination are degrees, arcminutes, and arcseconds. At a distance of 4.5 Mpc, 1 mJy = 2.41×10^{25} ergs s^{-1} Hz^{-1} (Thim et al. 2003). SN 1968L is located in the confused nuclear region of the galaxy. We were unable to get meaningful limits for either radio or X-ray luminosities.

[a] Value given is the 3 σ upper limit for 0.3–8 keV.

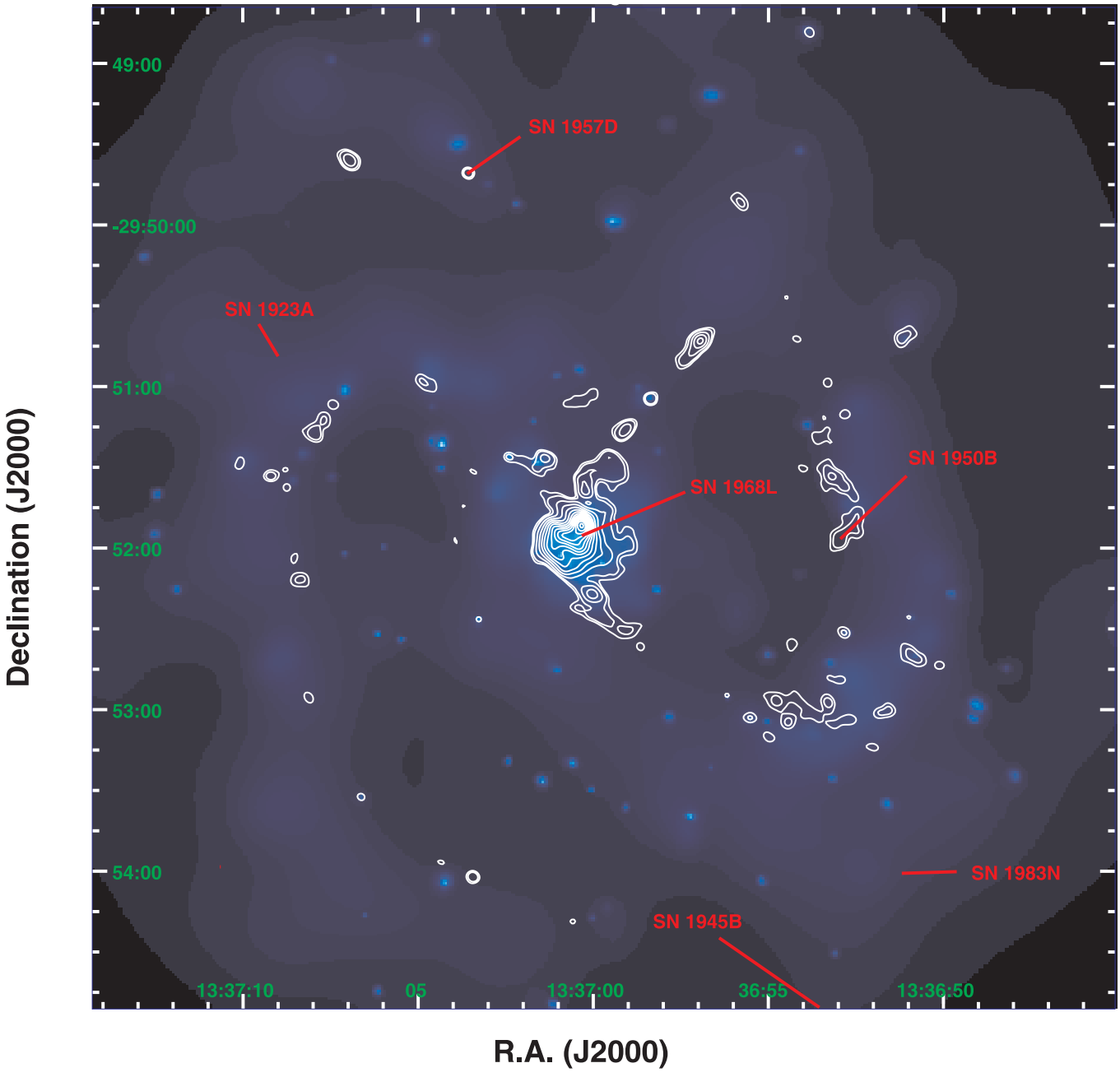

FIG. 1.—Radio contours (20 cm; 1998) overlaying the soft X-ray (0.3–2 keV; 2001) image of M83.

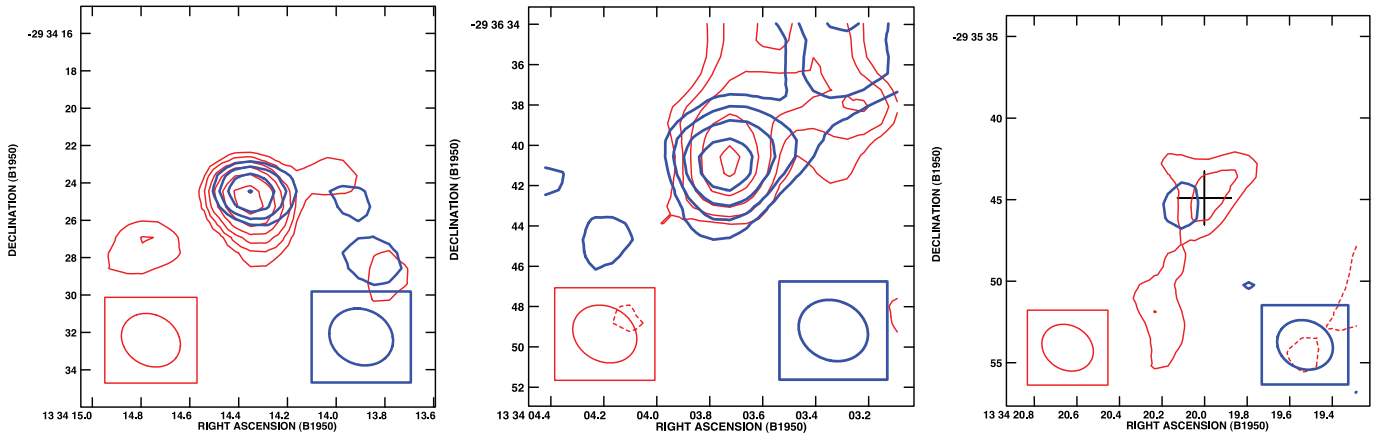

FIG. 2.—Radio contour images at 20 cm (*red lines*) and 6 cm (*blue lines*) of SNe 1957D, 1950B, and 1923A (*left to right*). Contour levels at both wavelengths are −0.12, 0.12, 0.17, 0.24, 0.34, 0.48, 0.68, and 0.96 mJy beam^{-1}. At 20 cm, the beam size is shown in the lower left, and at 6 cm, the beam size is shown in the lower right.

sidelobes from the brightest emission in the nucleus. The use of this algorithm allowed us to reduce the noise and to detect many faint sources. Uncertainties in the peak intensities are reported as the rms noise from the observations. At 20 cm the beam size is $3\farcs67 \times 3\farcs13$, P.A. $= 63\fdg58$, and the rms noise is 0.040 mJy beam^{-1}. At 6 cm the beam size is $3\farcs52 \times 3\farcs16$, P.A. $= 273\fdg0$, and the rms noise is 0.037 mJy beam^{-1}. The results of our analyses of the 1998 positions and peak flux densities are presented in Table 1 and Figure 1. All flux density measurements were made with the AIPS routine IMFIT using a two-component model, a two-dimensional Gaussian component, and a linear sloping background component, which was the model used by Cowan et al. (1994). The errors reported with the flux measurements and the positions were also determined by IMFIT. The previous work of Cowan et al. (1994) and Cowan & Branch (1985) was also re-reduced and re-imaged with the same techniques used for the 1998 data. To aid in the identification and modeling of point sources, the 20 cm data taken in 1983 and 1992 were deconvolved using restoring beams similar in shape to the 1998 data (rather than the highly elliptical beams derived by SCIMG). A more detailed description of the data reduction of the earlier observations will be presented in L. A. Maddox et al. (2006, in preparation).

2.2. *X-Ray*

M83 has been observed twice with *Chandra* using ACIS-S. The first observation was a 50 ks exposure in 2000 April (ObsID 793) and the second a 10 ks observation in 2001 September (ObsID 2064). These observations have been reduced as described by Kilgard et al. (2005). No X-ray sources were detected at the positions of historical SNe in either exposure (Soria & Wu 2002; Kilgard et al. 2005). Upper limits to the 0.3–8 keV X-ray luminosity are given in Table 1. The upper limits were derived from the longer observation (ObsID 793) by integrating the number of valid X-ray counts in a 5″ aperture centered on the position of the SNe. Typically, 10–20 X-ray counts were obtained at each position. Since most of the counts are likely to be diffuse background intrinsic to the galaxy, the luminosities in Table 1 are hard upper limits.

3. RESULTS AND DISCUSSION

3.1. *Radio Emission from Historical Supernovae*

With the VLA observations in 1998, we detected radio emission from the sites of SNe 1923A, 1950B, and 1957D at 20 and 6 cm, coincident within the error limits of the sources detected by Cowan et al. (1994) and Eck et al. (1998). No radio emission was detected from SNe 1945B, 1968L, and 1983N, and the implications of these nondetections are discussed at the end of this section. The measured flux densities at 20 and 6 cm (presented in Table 1) indicate a decrease from 1992 to 1998 for SN 1957D but no significant changes for SNe 1923A and 1950B. SN 1957D faded by 58% at both observed wavelengths from the prior observations in the early 1990s.

As indicated in Table 1 (and shown in Figs. 1 and 2), our new observations indicate that the spectral indices (α; $S \propto \nu^{\alpha}$) for both SNe 1923A and 1950B are flat. Our reanalysis of the results of Eck et al. (1998) and Cowan et al. (1994) indicate that the spectral indices of both SN 1923A and SN 1950B are unchanged between the early and late 1990s. Assuming both were correctly identified as SNe, the typical model for radio emission predicts a steadily decreasing, nonthermal emission (Weiler et al. 2002). In the case of these SNe, their radio emission is likely already at or below the level of the thermal emission from an intervening H II region along the line of sight (Montes et al. 1997). SN 1957D, however, remains nonthermal and continues to fade at both wavelengths, as predicted by the models of Weiler et al. (1986, 1990, 2002). The evolution of these three SNe is consistent with the theoretical models of Weiler et al. (1986, 1990, 2002) and Montes et al. (1997) for radio SNe in which the 6 cm light curve peaks before the 20 cm emission.

The observed radio properties of SNe 1923A, 1950B, and 1957D are typical of values reported for other radio SNe (see Fig. 3). It is clear, for example, from Figure 3 that the inferred radio luminosities of SNe 1957D and 1950B are (at a similar age of $\simeq$30–40 yr) very similar to the luminosities of SN 1961V in NGC 1058 and SN 1970G in M101 at the same stage in their evolution. This correlation in luminosity also lends credence to our identification of SN 1950B as a Type II SN. There is no reliable spectrum or optical light curve of SN 1950B to make a definitive classification as a Type II SN. In particular, there has been some uncertainty in the optical position of SN 1950B that prevented a conclusive identification of the SN with the radio source (Cowan & Branch 1985; Cowan et al. 1994).

The evolution of the radio flux density of SNe 1923A, 1950B, and 1957D is also consistent with the current models for radio emission from SNe, which predict a general decline in radio luminosity with age and declining density of CSM. Figure 3 illustrates that trend for a number of decades-old radio SNe, with a gradual fading of the radio light curves 10 yr after the SN event. Data, fits, and distances for SNe 1923A, 1950B, and

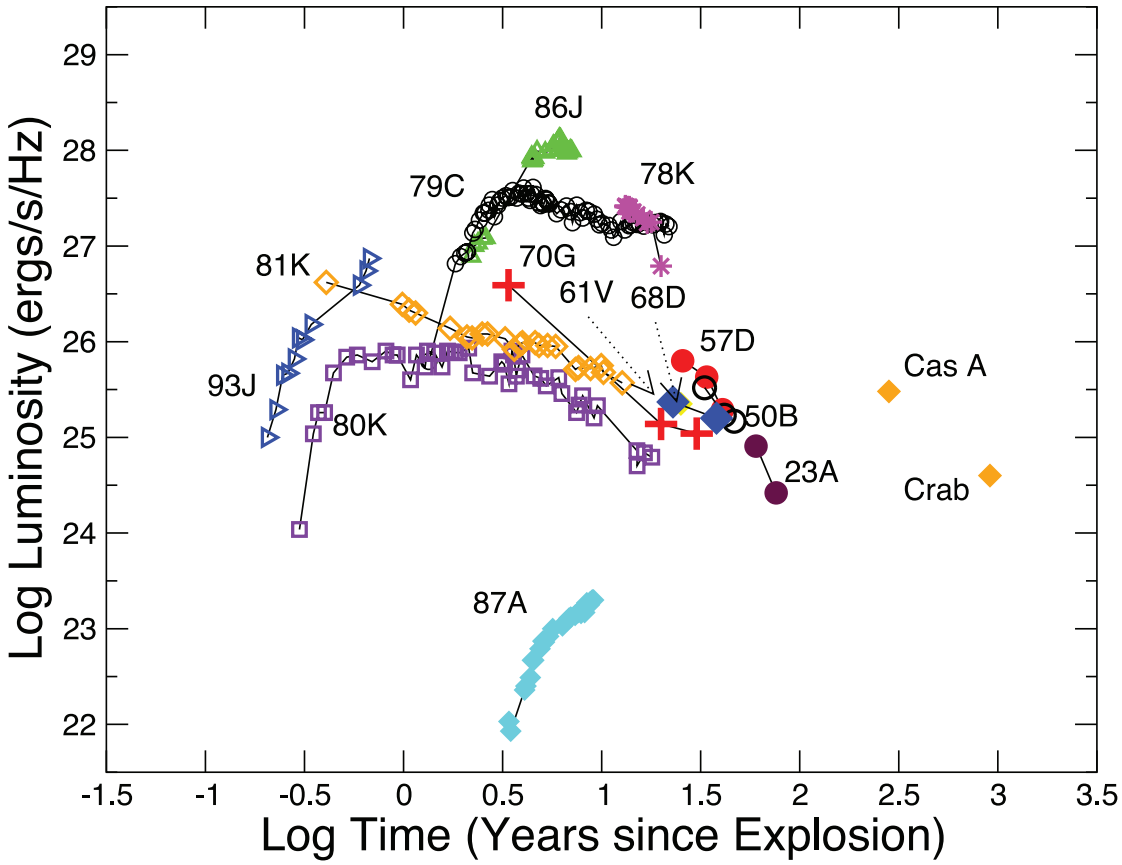

FIG. 3.—The 20 cm radio light curve of several radio SNe II and SNRs. Data and distances are shown for SNe 1923A (*maroon filled circle and maroon, open, inverted triangle for upper limit*), 1950B (*black open circles*), 1957D (*red filled circles*), SN 1961V (*blue filled diamonds*), SN 1968D (*yellow filled diamond*), SN 1970G (*red crosses*), SN 1978K (*magenta asterisks*), SN 1979C (*black open circles*), SN 1980K (*purple open squares*), SN 1981K (*orange open diamonds*), SN 1986J (*green triangles*), SN 1987A (*cyan filled diamonds*), and SN 1993J (*blue open triangles*). Luminosities for Cas A and the Crab (*orange filled diamonds*) are also shown.

1957D are taken from this paper and Thim et al. (2003), and for SN 1961V (Stockdale et al. 2001b; Silbermann et al. 1996), SN 1968D (Hyman et al. 1995; Tully 1988), SN 1970G (Stockdale et al. 2001a; Cowan et al. 1991; Kelson et al. 1996), SN 1978K (Ryder et al. 1993; Schlegel et al. 1999; Tully 1988), SN 1979C (Weiler et al. 1986, 1991; Montes et al. 2000; Ferrarese et al. 1996), SN 1980K (Weiler et al. 1986, 1992; Montes et al. 1998; Tully 1988), SN 1981K (van Dyk et al. 1992; Freedman et al. 2001), SN 1986J (Rupen et al. 1987; Weiler et al. 1990; Silbermann et al. 1996), SN 1987A (Ball et al. 1995; Mitchell et al. 2001), SN 1993J (van Dyk et al. 1994; Freedman et al. 2001), and Cas A and the Crab (Eck et al. 1998).

The differences in the behavior of the individual SNe are likely explained in terms of the density of the material encountered by the SN shock. Thus, for example, the shocks associated with some radio SNe (e.g., SNe 1979C, 1970G, and 1961V and early observations of SN 1950B) might be traveling through considerably denser CSM than other similarly aged radio SNe (e.g., SNe 1980K, 1978K, 1957D, and 1923A). Consistent with this interpretation is the very rapid decline in the radio emissions of Type Ib radio SNe, e.g., SNe 1983N and 1984L, which presumably have lower density CSM (Weiler et al. 1986; Sramek et al. 1984; Panagia et al. 1986).

One scenario that might explain an increased density of CSM around some Type II radio SNe could be that the progenitors underwent large-scale eruptions, akin to luminous blue variables (LBVs), prior to the SN event. The mass-loss rates during an LBV eruption can be 10–100 times larger than the typical supergiant mass-loss rate (Humphreys & Davidson 1994). The exact epoch at which this may have occurred depends on the ejection velocities of the CSM during these events, the rate of expansion of the SN shock, and the density of the CSM. Unfortunately, these objects are too undersampled to make any definitive statements as to the exact nature of such a possible outburst or mass loss. Clearly, additional radio monitoring of SNe 1957D, 1950B, 1923A, and other radio SNe will be important in understanding the continuing evolution and nature of these relatively rare objects.

The 1998 observations detected no radio emission from SNe 1945B, 1968L, and 1983N. SNe 1945B and 1968L have never been detected in the radio. SN 1945B is located along a spiral arm, and nothing can be inferred by its nondetection, as very little is known about this SN (Liller 1990). SN 1968L is located within a region of diffuse radio emission (background level $\simeq$3 mJy) in the nuclear region of M83. SN 1983N was detected by Cowan & Branch (1985) within 1 yr after discovery with flux densities at 20 and 6 cm of 4.1 $\pm$ 0.1 and 0.70 $\pm$ 0.06 mJy, respectively, the brightest historical radio SN detected in M83. SN 1983N was likely a Type Ib SN and is not expected to be a detectable radio source at this epoch, as Type I SNe typically have very low density CSM (van Dyk et al. 1996; Weiler et al. 2002). SN 1968L would need to have been at least 3 times more luminous 15 yr after explosion than SN 1983N (in the 1983 epoch) to have been detectable in the 1983 observations and in subsequent observations in the 1990s. The diffuse nuclear radio emission coupled with the age of SN 1968L make it highly unlikely that it will ever be detected in the radio at the 1″ resolution scale. Very long

baseline interferometric (VLBI) observations have been made to study the nuclear region and search for radio emission from SN 1968L using the Long Baseline Array of the Australia Telescope National Facility. These results will be presented in a later publication.

3.2. *X-Ray Constraints on Historical SNe*

Using the deep *Chandra* observation, we can put tight constraints on the X-ray emission and CSM properties of the historical SNe in M83. Assuming a thermal plasma emission with a temperature of $kT = 0.8$ keV, typical for the late emission originating in a reverse shock, the upper limits to the (0.3–8 keV) X-ray luminosity are a few times 10^{36} ergs s^{-1} (3 σ; see Table 1). If the CSM densities are dominated by the winds blown by the progenitor stars of the SNe, we can use the X-ray interaction luminosity

$$L_{\rm X} = \frac{4}{\left(\pi m_{\rm H+He}^2\right)\Lambda(T)\left(\dot{M}/v_w\right)^2}(v_s t)^{-1}$$

at time t after the outburst to measure the ratio $\dot{M}/v_w$ (Immler & Lewin 2003). Assuming that v_w does not change over time, we can even directly estimate the mass-loss rates of the progenitors.

For each of the SNe we estimate mass-loss rates of $\dot{M} \approx (10^{-8}\ M_\odot\ {\rm yr}^{-1})(v_w/10\ {\rm km\ s}^{-1})$. Progenitors of Type II SNe following core collapse of massive stars have high mass-loss rates ($\dot{M} \sim 10^{-4}$ to $10^{-6}\ M_\odot\ {\rm yr}^{-1}$) and low wind velocities of typically $v_w \sim 10\ {\rm km\ s}^{-1}$. Type Ib/c SNe have lower mass-loss rates ($\dot{M} \sim 10^{-5}$ to $10^{-7}\ M_\odot\ {\rm yr}^{-1}$) and significantly higher wind velocities of 10 km s$^{-1} < v_w \lesssim 1000$ km s^{-1}.

Our inferred mass-loss rates are consistent with previous observations of other decades-old SNe. SN 1980K was reported with an X-ray luminosity of 3.1×10^{37} ergs s^{-1}, measured with *ROSAT* in 1992 in the 0.1–2.4 keV range, and was not detected in *Chandra* observations in 2001 with a limiting detection threshold of $\sim 10^{37}$ ergs s^{-1} in the 0.3–5 keV range (Schlegel 1994; Holt et al. 2003). There have been numerous X-ray SNe detected with $L_{\rm X} \sim 10^{38}-10^{41}$ ergs s^{-1}, and there has been a clear correlation between their X-ray and radio luminosities in the first 10 yr following the SN explosion (Pooley et al. 2002). No X-ray emission has been detected from SNe with ages comparable to those of SNe 1957D, 1950B, and 1923A, with upper limits established for SN 1959D (in NGC 7331) of 1.2×10^{38} ergs s^{-1} and for SN 1961V (in NGC 1058) of 1.5×10^{40} ergs s^{-1} (Stockdale et al. 1998a, 1998b).

Each X-ray observation at time t is related to the corresponding distance r from the site of the explosion, $r = v_s t$ (with shock front velocity v_s), and to the age of the stellar wind, $t_w = t v_s/v_w$. The *Chandra* measurements decades after the outbursts of the historical SNe in M83 probe the CSM at large radii ($>10^{18}$ cm) from the sites of the explosions. The observed lack of significant X-ray emission is due to the lack of shocked CSM originating in the low-density stellar winds of the progenitors.

4. SUMMARY

M83 serves as an excellent laboratory to study decades-old SNe as they transition into SNRs. The 15 year study by Cowan and collaborators has provided valuable insight into the evolution of these historical SNe and the nature of their environment. We report the continued decline in the nonthermal radio emission from SN 1957D and the apparent fading of SNe 1923A and 1950B below the confusion level of associated or intervening H II regions. We further report that SN 1983N was not detected in the latter epochs since its initial discovery in 1983, and its behavior is typical of Type Ib and Ic SNe. The radio nondetections of SNe 1945B and 1968L are also noted, although very little can be inferred from these results due to lack of information about these sources and (in the case of SN 1968L) the strong diffuse emission in the nuclear region of M83. Finally, we report the X-ray nondetection of all six historical SNe with *Chandra*. These results place more stringent constraints on the mass-loss rates of the progenitors than was previously possible. VLA observations are needed to explore the radio emission in these decades-old SNe and to continue to chart their evolution from SNe into SNRs.

We thank Michael P. Rupen for his assistance in imaging the 20 cm 1998 VLA data, Christina Lacey, who was the principle investigator for the 1998 radio observations, and Emily Wolfing for her contributions through the NSF/REU program at the University of Oklahoma. We also express our appreciation to the anonymous referee, whose comments were very useful in improving this manuscript. The research was supported in part by the NSF (AST 03-07279 to J. J. C.), a *Chandra* grant (GO1-2092B), the NASA Wisconsin Space Grant Consortium (C. J. S.), and an award from the Research Corporation (C. S. is a Cottrell Scholar). We have made use of the NASA/IPAC Extragalactic Database, which is operated by the Jet Propulsion Laboratory, California Institute of Technology, under contract with the National Aeronautics and Space Administration, and have made use of the new NRAO Data Archival Service.

REFERENCES

Ball, L., Campbell-Wilson, D., Crawford, D. F., & Turtle, A. J. 1995, ApJ, 453, 864
Chevalier, R. A. 1984, ApJ, 285, L63
Cowan, J. J., & Branch, D. 1982, ApJ, 258, 31
———. 1985, ApJ, 293, 400
Cowan, J. J., Goss, W. M., & Sramek, R. A. 1991, ApJ, 379, L49
Cowan, J. J., Roberts, D. A., & Branch, D. 1994, ApJ, 434, 128
Cowsik, R., & Sarkar, S. 1984, MNRAS, 207, 745
de Vaucouleurs, G. 1979, AJ, 84, 1270
Eck, C. R., Roberts, D. A., Cowan, J. J., & Branch, D. 1998, ApJ, 508, 664
Ferrarese, L., et al. 1996, ApJ, 464, 568
Freedman, W. L., et al. 2001, ApJ, 553, 47
Holt, S. S., Schlegel, E. M., Hwang, U., & Petre, R. 2003, ApJ, 588, 792
Humphreys, R. M., & Davidson, K. 1994, PASP, 106, 1025
Hyman, S. D., van Dyk, S. D., Weiler, K. W., & Sramek, R. A. 1995, ApJ, 443, L77
Immler, S., & Lewin, W. H. G. 2003, in Supernovae and Gamma-Ray Bursters, ed. K. W. Weiler (Berlin: Springer), 91
Immler, S., Vogler, A., Ehle, M., & Pietsch, W. 1999, A&A, 352, 415
Kelson, D. D., et al. 1996, ApJ, 463, 26
Kilgard, R. E., et al. 2005, ApJS, 159, 214
Liller, W. 1990, IAU Circ., 5091, 2
Mitchell, R. C., Baron, E., Branch, D., Lundqvist, P., Blinnikov, S., Hauschildt, P. H., & Pun, C. S. J. 2001, ApJ, 556, 979
Montes, M. J., van Dyk, S. D., Weiler, K. W., Sramek, R. A., & Panagia, N. 1998, ApJ, 506, 874
Montes, M. J., Weiler, K. W., & Panagia, N. 1997, ApJ, 488, 792
Montes, M. J., Weiler, K. W., Van Dyk, S. D., Panagia, N., Lacey, C. K., Sramek, R. A., & Park, R. 2000, ApJ, 532, 1124
Panagia, N., Sramek, R. A., & Weiler, K. W. 1986, ApJ, 300, L55
Pooley, D., et al. 2002, ApJ, 572, 932
Rupen, M. P., van Gorkom, J. H., Knapp, G. R., Gunn, J. E., & Schneider, D. P. 1987, AJ, 94, 61
Ryder, S., Staveley-Smith, L., Dopita, M., Petre, R., Colbert, E., Malin, D., & Schlegel, E. 1993, ApJ, 416, 167

Sandage, A., & Tammann, G. A. 1987, Revised Shapley-Ames Catalog of Bright Galaxies (2nd ed.; Washington: Carnegie Inst.)
Schlegel, E. M. 1994, AJ, 108, 1893
Schlegel, E. M., Ryder, S., Staveley-Smith, L., Petre, R., Colbert, E., Dopita, M., & Campbell-Wilson, D. 1999, AJ, 118, 2689
Silbermann, N. A., et al. 1996, ApJ, 470, 1
Soria, R., & Wu, K. 2002, A&A, 384, 99
Sramek, R. A., Panagia, N., & Weiler, K. W. 1984, ApJ, 285, L59
Stockdale, C. J., Cowan, J. J., & Romanishin, W. 1998a, BAAS, 30, 1260
Stockdale, C. J., Goss, W. M., Cowan, J. J., & Sramek, R. A. 2001a, ApJ, 559, L139
Stockdale, C. J., Romanishin, W., & Cowan, J. J. 1998b, ApJ, 508, L33
Stockdale, C. J., Rupen, M. P., Cowan, J. J., Chu, Y., & Jones, S. S. 2001b, AJ, 122, 283
Talbot, R. J., Jensen, E. B., & Dufour, R. J. 1979, ApJ, 229, 91
Thim, F., Tammann, G. A., Saha, A., Dolphin, A., Sandage, A., Tolstoy, E., & Labhardt, L. 2003, ApJ, 590, 256
Tully, R. B. 1988, Nearby Galaxies Catalog (Cambridge: Cambridge Univ. Press)
van Dyk, S. D., Hamuy, M., & Filippenko, A. V. 1996, AJ, 111, 2017
van Dyk, S. D., Weiler, K. W., Sramek, R. A., & Panagia, N. 1992, ApJ, 396, 195
van Dyk, S. D., Weiler, K. W., Sramek, R. A., Rupen, M. P., & Panagia, N. 1994, ApJ, 432, L115
Weiler, K. W., Panagia, N., Montes, M. J., & Sramek, R. A. 2002, ARA&A, 40, 387
Weiler, K. W., Panagia, N., & Sramek, R. A. 1990, ApJ, 364, 611
Weiler, K. W., Sramek, R. A., Panagia, N., van der Hulst, J. M., & Salvati, M. 1986, ApJ, 301, 790
Weiler, K. W., van Dyk, S. D., Discenna, J. L., Panagia, N., & Sramek, R. A. 1991, ApJ, 380, 161
Weiler, K. W., van Dyk, S. D., Panagia, N., & Sramek, R. A. 1992, ApJ, 398, 248